Journal of the European Ceramic Society 20 (2000) 1677–1686

Improvement of calcium modified lead titanate piezoceramics by hot isostatic pressing

J. Ricote *, L. Pardo

Instituto de Ciencia de Materiales de Madrid, CSIC, Cantoblanco, 28049 Madrid, Spain

Received 14 September 1999; accepted 3 January 2000

Abstract

The hot isostatic pressing (HIP) is used in this work as a post-sintering treatment to obtain piezoelectric ceramics with very low contents of porosity. The method is applied to calcium modified lead titanate ceramics with a wide range of microstructures, corresponding to successive sintering stages. The effects of HIP on the various cases are quantitatively determined, checking the effectiveness of the treatment to reduce the porosity without further grain growth. A combination of computer-aided image processing and measurement with optical and scanning electron (SEM) micrographs and transmission electron microscopy (TEM) are used to characterise the microstructures. The effect of HIP on the porosity is different depending on the sintering stage of the ceramic. Their ferropiezoelectric behaviour is also evaluated in relation to the microstructural changes.

Keywords: Ferroelectric properties; Grain size; Hot isostatic pressing; (Pb; Ca)TiO_3; Porosity

1. Introduction

The hot isostatic pressing (HIP) is routinely used to obtain ceramics with very low contents of porosity in high performance engineering ceramics and bioceramics. HIP as a post-sintering treatment has been used in the processing of piezoelectric ceramics.[1,2] However, and despite its interest, the effort devoted to the study of HIP in piezoceramics is scarce.

Calcium and rare earth modified lead titanate ceramics exhibit very interesting electromechanical properties, like a high linearity of the piezoelectric response and an unusually large anisotropy of the piezoelectric coefficients,[3] which has resulted in extensive research on these compositions to understand these phenomena. These special features make modified lead titanate ceramics good candidates for applications in high frequency bulk[4] and surface acoustic wave (SAW) devices,[5] among others. For both types of applications the scattering of acoustic waves by grains and pores is a key issue, as it is the source of propagation losses, which must be reduced by control of the ceramic microstructure during processing. HIP, as a post-sintering treatment, has been applied[6–9] to modified lead titanate piezoelectric ceramics with relatively low porosity contents and in the final stage of sintering, i.e., with small isolated pores. In that case, a spectacular reduction of the porosity takes place and porosity contents of less than 1% can be achieved, without significant increase of the grain size. In this way it was successfully improved the piezoelectric performance as bulk transducers[7,8] and as SAW devices[9] by increasing the free surface velocity and the surface coupling coefficient and reducing the propagation losses.

The question is whether the sintered microstructure is a limiting factor to obtain better piezoelectric ceramics or not, and if so to what extend. It was already pointed out[10] the importance of the type of porosity in the achievement of further densification of Al_2O_3 ceramics. Nevertheless, that work does not consider other factors that can also be affected and determine the performance of the material, like the grain size seems to be for high frequency bulk and SAW applications. This systematic study of the HIP effect on the microstructure and properties of lead titanate based ferroelectric ceramics with different sintering stages aims to assess its effectiveness to produce materials with improved properties

* Corresponding author.

0955-2219/00/$ - see front matter
PII: S0955-2219(00)00042-X

for piezoelectric applications and will shed light on the mechanisms that intervene in the densification process.

A series of Ca modified lead titanate ceramics with a wide range of microstructures were HIP treated, and the changes in their porosity and grain size quantitatively determined. The use of computer-aided processing and measurements of images from microscopy and a graphic method to study the size distributions provide new and useful information in the processing of piezoceramics. To complete the microstructural study, information from a deeper level, such as the ferroelectric domain configuration, is obtained by transmission electron microscopy (TEM). The ferro-piezoelectric properties are also measured and correlated to the microstructural changes observed.

2. Experimental procedure

2.1. Materials preparation and characterisation

Calcium modified lead titanate ceramics with nominal composition:

$$Pb_{0.74}Ca_{0.26}\left[(Co_{0.5}W_{0.5})_{0.05}Ti_{0.95}\right]O_3 + 1\%MnO$$

were prepared by a method reported elsewhere,[11] under different sintering conditions: 1000°C for 3 h (PTC-1); 1000°C-5 h (PTC-2); 1050°C-3 h (PTC-3); 1050°C-5 h (PTC-4); 1100°C-3 h (PTC-5); and 1100°C-5 h (PTC-6). Then some of the sintered pellets were hot isostatically pressed, without encapsulation, in an atmosphere of 20% O_2 and 80% Ar at a pressure of 100 MPa, at 1000°C for 17 hours. Heating and cooling rates were 600°C/h.

The tetragonal distortion of the perovskite type structure (c/a) of the ceramics was analysed by X-ray diffraction (XRD). Quantitative Energy Dispersive Spectroscopy (EDS) was used to study the final composition of ceramics.

2.2. Microstructural characterisation

The porosity contents and the pore size distributions were determined by computer-aided image analysis of optical micrographs from polished surfaces. The grain size distributions were obtained by scanning electron microscopy (SEM) of polished and thermally etched surfaces. The image analysis was carried out using software based on IMCO10-KAT386 system (Kontron Elektronik GMBH 1990) as reported elsewhere.[6,12] The porosity is quantified by the fractional area occupied by pores in the image. The equivalent diameter to a circular shape was chosen as the parameter to quantify grain sizes. This is defined as $G = (4.A/\pi)^{1/2}$, where A is the area inside the grain. The type of distributions obtained were analysed by a graphic method using probability plots.[13] The average values and standard deviations were calculated by linear fitting of these experimental data in probability plots. The mixture of two distribution functions, i.e. bimodal distributions, was detected by changes in the slope of the curves, and the two distributions, called parent distributions analysed separately.

Specimens for transmission electron microscopy (TEM) were prepared from 3 mm discs, which were mechanically polished up to ~200 μm thickness and then dimpled in the centre of the disc to ~20 μm. This was followed by further thinning to the electron transparency by Ar^+ ion milling, with a voltage of 5 kV and an incident angle of 15°. Observations were carried out with a Philips CM20 microscope working at 200 kV.

2.3. Dielectric and piezoelectric characterisation

For the dielectric and piezoelectric measurements, thickness-poled rectangular bars, with length to width and thickness ratio higher than 3:1, were prepared from sintered pellets. The d_{33} piezoelectric coefficient was measured in a Berlincourt piezo-meter. The dielectric permittivity, ε_{33}^{T}, and losses, $\tan\delta$, at 1 kHz were measured in an HP4192A LF impedance analyser. The electromechanical coupling factor k_{31}, and the elastic compliance s_{11}^{E} were calculated with high accuracy by an automatic iterative procedure.[14]

3. Experimental results and discussion

The tetragonal distortion of the perovskite structure (c/a) obtained by XRD does not change significantly from the as-sintered samples ($c/a = 1.038$) to the HIP treated ones ($c/a = 1.037$). The quantitative EDS analysis of these ceramics shows agreement with the nominal composition (Table 1). Differences among the concentration values of the majority elements are found insignificant. Therefore, we can conclude that the HIP treatment does not produce any relevant effect on the structure and composition of these ceramics, and then, the variations in the macroscopic properties induced by HIP can only be attributed to the microstructural changes produced during that treatment.

Micrographs showing the variety of microstructures of the HIP treated ceramics studied here are presented in Figs. 1 and 2. Fig. 1 contains SEM micrographs of etched surfaces revealing the grain size, while in Fig. 2 optical micrographs of polished surfaces show the porosity of the ceramics. From the computerised image analysis and measurements on series of micrographs of this type we obtain the porosity contents and the size distributions (Table 2). Their probability plots are shown in Figs. 3 and 4. For the sake of comparison the

Table 1
Element ratios obtained by the EDS analyses of HIP treated PTC ceramics, compared to the nominal composition ones

Ratio	Nominal composition	PTC-1 HIP	PTC-2 HIP	PTC-3 HIP	PTC-4 HIP	PTC-5 HIP	PTC-6 HIP
Pb/(Pb + Ca)	0.74	0.76	0.77	0.73	0.74	0.74	0.74
Ca/(Pb + Ca)	0.26	0.24	0.23	0.27	0.26	0.26	0.26
Ti/(Co + W + Ti)	0.95	0.96	0.96	0.97	0.97	0.96	0.97
W/(Co + W + Ti)	0.03	–	0.01	–	0.01	0.01	0.01
Co/(Co + W + Ti)	0.03	0.04	0.03	0.03	0.03	0.03	0.03
(Pb + Ca)/(Co + W + Ti)	1.00	1.07	1.05	0.97	0.99	0.99	0.99
Percentage of Mn	0.01	0.02	0.02	0.02	0.02	0.02	0.02

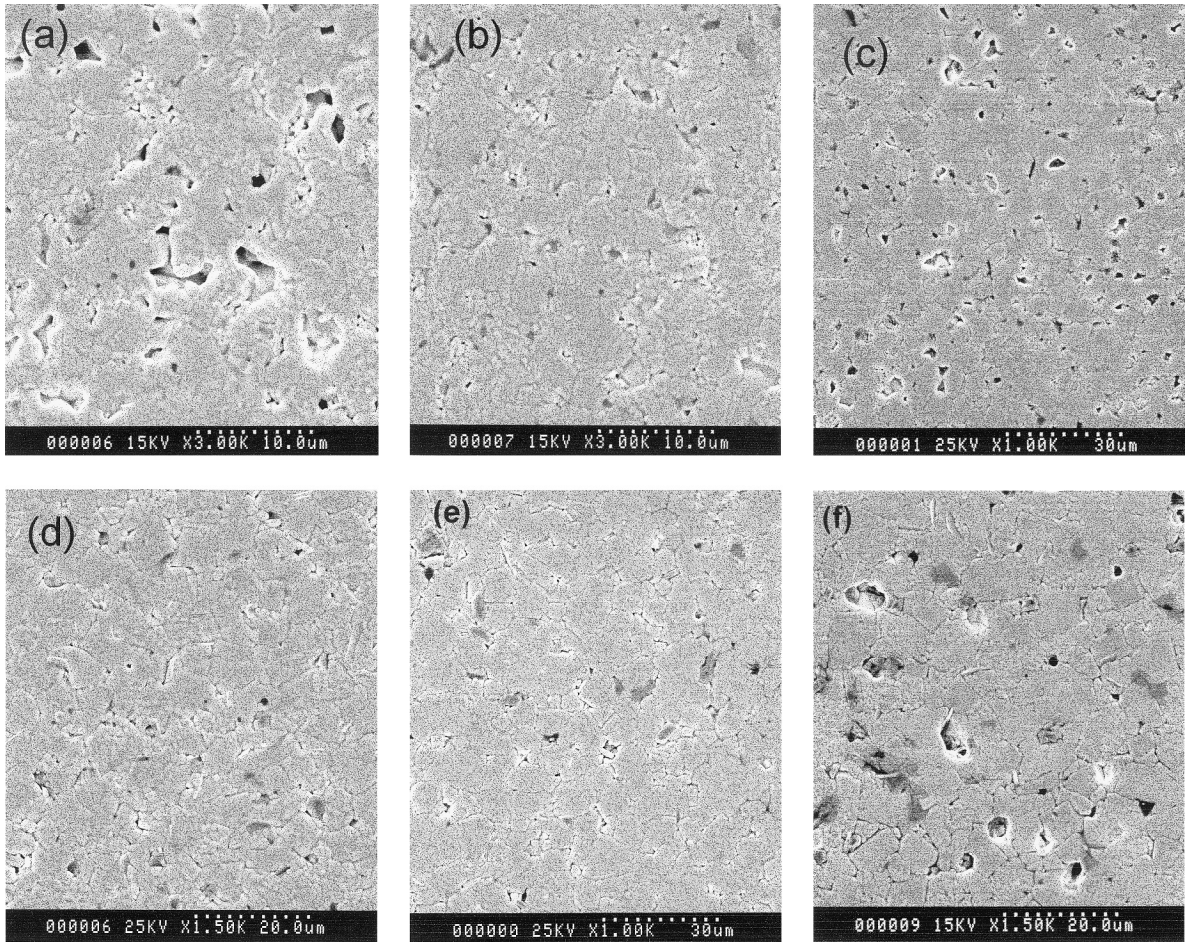

Fig. 1. SEM micrographs showing the grain size for HIP treated ceramics: (a) PTC-1 HIP; (b) PTC-2 HIP; (c) PTC-3 HIP; (d) PTC-4 HIP; (e) PTC-5 HIP; (f) PTC-6 HIP.

probability plots of the corresponding as-sintered samples[12] are also shown. A linear fitting is found for the experimental data of all the HIP treated ceramics, which reveals that the distributions are lognormal. Most of them are single functions, but some pore area distributions are bimodal. The average values and the standard deviations of the grain diameter (G and σ_G) and pore area distributions (P and σ_P), obtained from the probability plots, are summarised in Table 2, which also compares results of as-sintered and HIP treated ceramics.

Comparing the average values of the distributions and excluding the ceramics with the highest porosity (PTC-1 and -2), there is either a moderate increase or an insignificant change in the grain size [Table 2 and Fig. 3(c)–(f)]. The temperature of HIP is lower than the one used for sintering, and therefore, no further grain growth is expected.[6] However, the long time used (17 h) results in a moderate increase of the grain size. Grain size distributions are single lognormal functions for all the samples (Fig. 3), before and after HIP, showing that a process of normal grain growth has been followed for

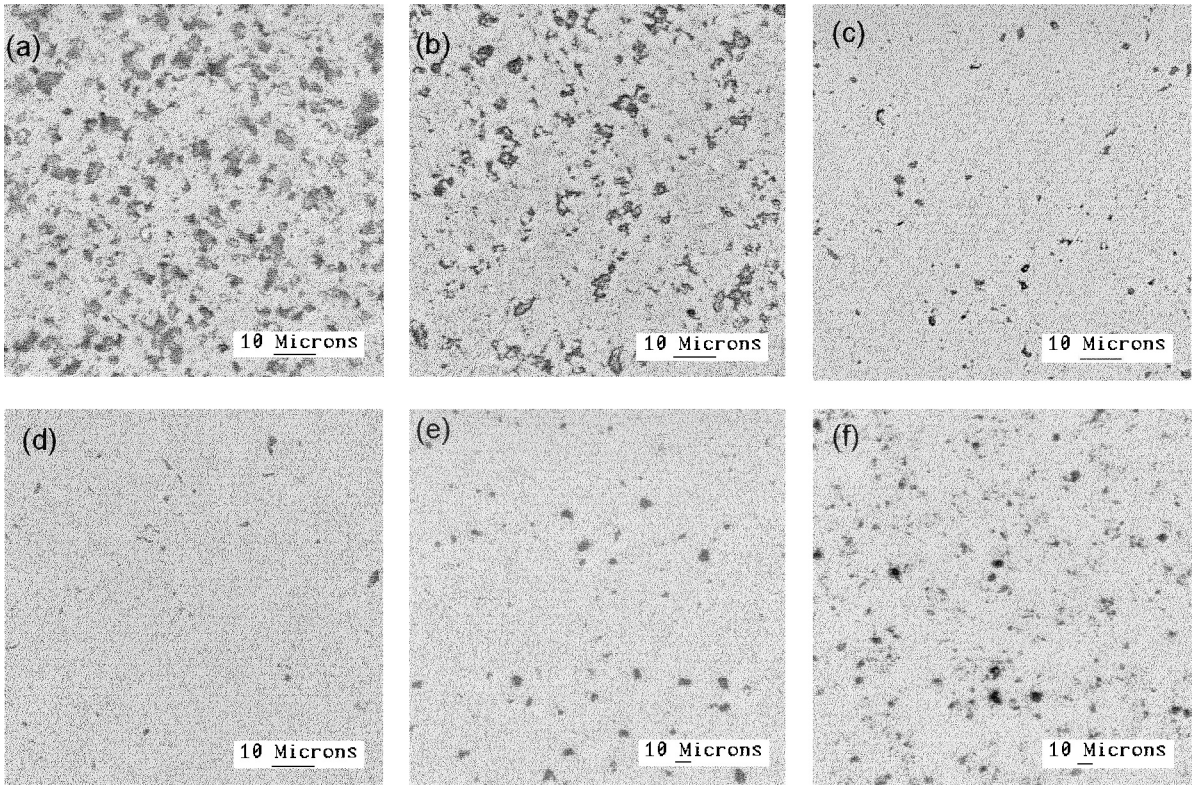

Fig. 2. Optical micrographs showing the porosity for HIP treated ceramics: (a) PTC-1 HIP; (b) PTC-2 HIP; (c) PTC-3 HIP; (d) PTC-4 HIP; (e) PTC-5 HIP; (f) PTC-6 HIP.

all of them. This means that the application of the HIP treatment does not produce preferential grain growth, which would result in bimodal distributions.

The main microstructural change induced by HIP is the reduction of the porosity content. However, the amount of this reduction strongly depends on the starting sample. In the as-sintered ceramics two advanced sintering stages were identified. The so-called intermediate sintering stage,[12] which contains a significant amount of porosity (~20%), is described as composed of small ($P\sim$ 3 μm^2), often interconnected, elongated pores. The smallest pores do not present this elongated shape and are isolated. These are the characteristics found for the as-sintered PTC-1 and 2 ceramics. As the results in Table 2 clearly indicates, HIP has a relatively small effect on ceramics with this type of microstructure, producing the lowest reduction of the porosity, which, however, cannot be considered negligible: up to 40% reduction in PTC-2. A similar result was obtained in Al_2O_3 ceramics,[10] but in that work the authors were not able to analyse the remarkable effect of the HIP on the pore size, which produces a bimodal pore area distribution [Fig. 4(a) and (b)]. This is the consequence of a different effect on the smallest isolated pores, whose size distribution shifts to lower pore area ($P\sim1\ \mu m^2$), and on the elongate-shaped ones, which remains unaltered.

The elongated pores observed are in fact a network of interconnected pores in the ceramic, which ultimately connect to the surface of the ceramic. As a result they are filled with air, which is pushed inside the ceramic on application of the high pressure during HIP, preventing them from shrinking, as it was previously observed in Al_2O_3 ceramics.[10] This explains that their size distribution is not affected, while the area of isolated pores is reduced. At the same time, the external applied pressure is transmitted inside the ceramic through this network of pores, and in the case that a closed pore is formed from them, this will have high-pressure gas trapped. As a result the individual grains are submitted to high tensions, which eventually can result in fracture. This scenario may explain the unexpected reduction of the grain size of PTC-1 and 2 after HIP. Instead of grain growth, these ceramics show fragments coming from the fracture of the initial grains. Lower values of the applied pressure and a shorter treatment time may eliminate this effect, preserving the desired reduction of the porosity content.

The second advanced sintering stage[6,12] occurs when all the pores become isolated, with a significant decrease of the total porosity (~5%). This is the so-called ideal final stage of sintering of the ceramic. This is the case of the as-sintered PTC-3 and 4 ceramics, which show the greater effect of the HIP treatment on the pore size distributions [Table 2 and Fig. 4(c) and (d)]: up to 85% reduction of the porosity in PTC-4, giving place to the lowest porosity (0.7%) and pore area ($P=0.7\ \mu m^2$) after HIP.

Table 2
Average values and standard deviations of the grain diameter and the pore area distributions, together with the porosity content, for both as-sintered and HIP treated ceramics

PTC ceramic		Grain diameter		Pore area		Porosity (%)
		G (μm)	σ_G (μm)	P (μm^2)	σ_P (μm^2)	
PTC-1	Sintered	2.1	1.5	3.0	7.2	23.6
				Parent disributions		
	HIP	1.5	0.9	1.1	2.5	21.2
				3.0	7.2	
PTC-2	Sintered	2.3	1.4	3.0	6.9	18.7
				Parent distributions		
	HIP	1.5	0.8	0.9	2.2	11.3
				3.0	6.9	
PTC-3	Sintered	3.1	1.5	5.0	7.4	7.7
	HIP	4.3	2.2	0.9	1.8	3.4
PTC-4	Sintered	3.3	1.6	2.9	4.7	4.7
	HIP	3.6	2.1	0.7	0.9	0.7
				Parent distributions		
PTC-5	Sintered	4.5	2.6	5.0	7.4	10.8
				17.0	16.5	
				Parent distributions		
	HIP	5.2	2.8	1.6	2.8	1.8
				3.4	5.1	
				Parent distributions		
PTC-6	Sintered	3.9	2.1	2.9	4.7	16.3
				16.6	30.9	
				Parent distributions		
	HIP	3.3	2.0	1.0	1.8	3.1
				2.9	4.7	

The ceramics sintered at the highest temperatures, PTC-5 and PTC-6, present a so-called deteriorated final sintering stage, also previously identified and reported.[6,12] This is characterised by bimodal pore area distributions [Fig. 4(e) and (f)], caused by the appearance of very large ($P \sim 15$ μm^2) isolated pores. The number of these large pores is reduced during the HIP treatment, as can be deduced from the comparison of the corresponding probability plots in Fig. 4 (e) and (f). The value of the pore area for cumulative frequency of 50% is the Ln of the median, Ln (median) = M, and it is an appropriate parameter to show the evolution of these bimodal distributions. It can be seen that the shift of the medians is higher for the parent distributions of large pores, ΔM^{lp}, than those of the small pores, ΔM^{sp}. From this, we deduce the HIP treatment has a stronger effect on the larger pores, that allows to restore partially the deteriorated state of the microstructure, i.e. reducing the bimodal character of the pore distribution in the as-sintered sample.

All this reveals the importance, not only of the porosity value before HIP, but, also, of the initial sintering stage, i.e., the shape and size distribution of the pores, on the reduction of the porosity content by HIP.

Microstructural details at a deeper level can be obtained by TEM. Fig. 5 shows bright field images of ferroelectric domains for PTC-6 as-sintered and HIP. Both micrographs were taken viewing the grain along the [001] zone axis. The insets show the electron diffraction patterns. In both cases they exhibit a row of unsplit spots, while the rest are split in a direction parallel to this row and perpendicular to the (110) direction. This indicates the existence of (110) twin planes parallel to the electron beam.[15] After cooling from the paraelectric phase, ferroelectric crystals equilibrate the strains associated with the transition by the formation of dipolar domains, which are related to each other through twinning. In tetragonal ferroelectrics, the predicted planes corresponding to 90° domain walls are {110}. Therefore, the parallel lines observed in the micrographs, can be identified as (110) ferroelectric domain walls, separating bands of 90° domains. Apart from a small variation of the domain width which can be explained by differences in the size of the grain observed, the general aspect for both as-sintered and HIP samples does not show any significant changes. The HIP treatment seems not to affect the ferroelectric domain configuration of these materials. We can say

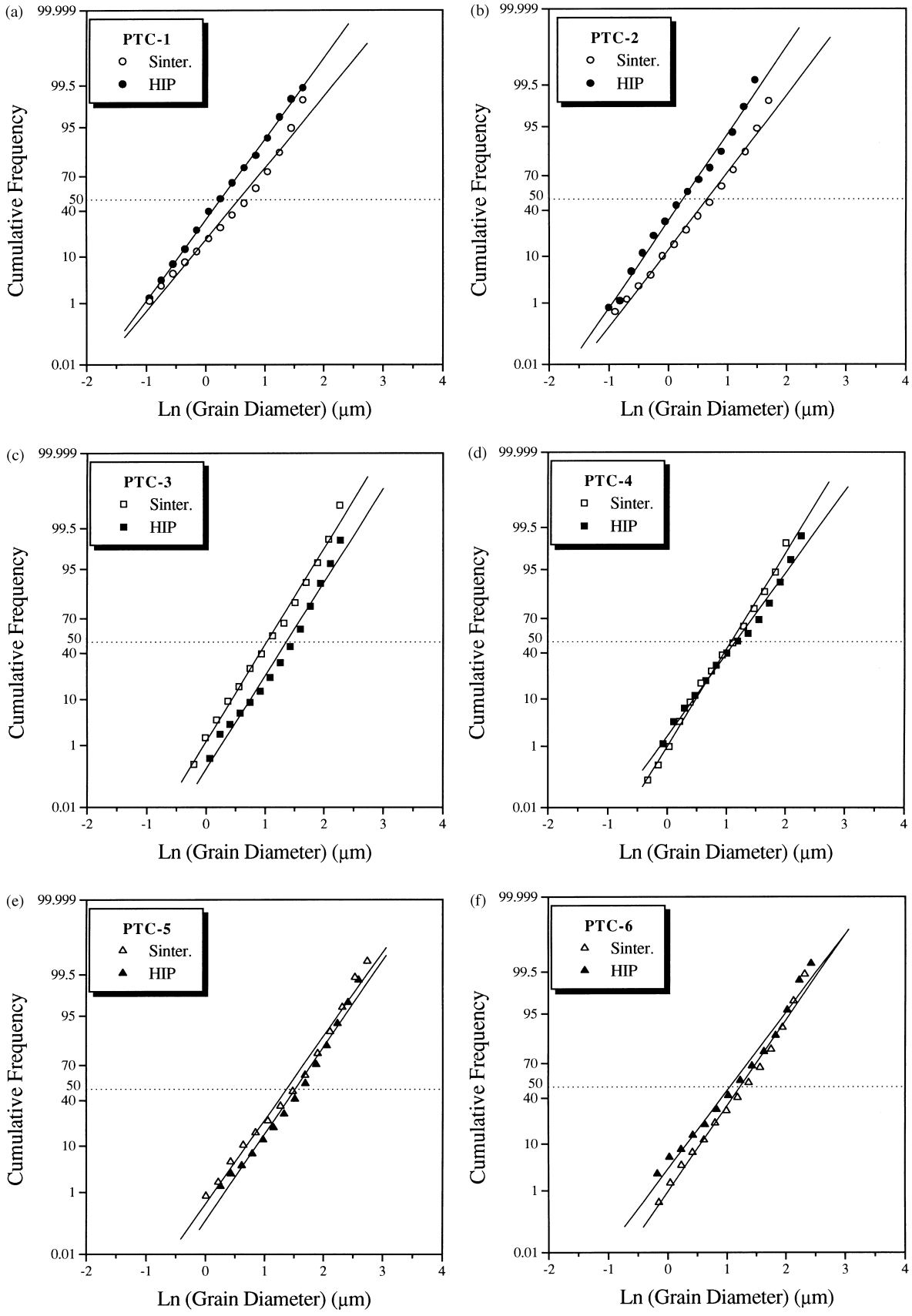

Fig. 3. Comparison between the probability plots of grain size distributions for as-sintered and HIP treated ceramics: (a) PTC-1; (b) PTC-2; (c) PTC-3; (d) PTC-4; (e) PTC-5; (f) PTC-6.

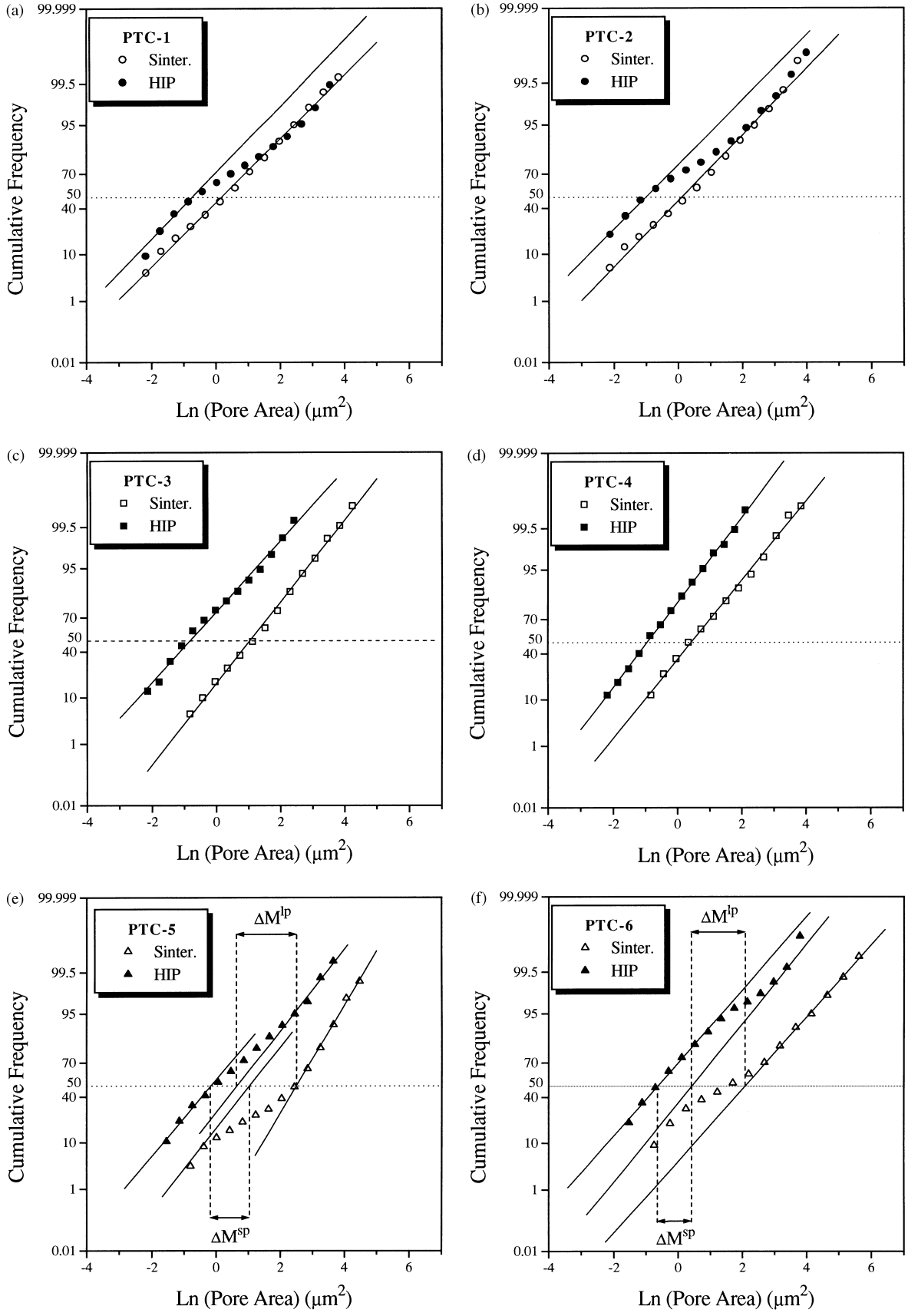

Fig. 4. Comparison between the probability plots of pore size distributions for as-sintered and HIP treated ceramics: (a) PTC-1; (b) PTC-2; (c) PTC-3; (d) PTC-4; (e) PTC-5; (f) PTC-6.

that it affects mainly the microstructural parameters at a mesoscopic scale (porosity and grain size) and those will be responsible of the possible variations of the ferropiezoelectric behaviour of the HIP treated ceramics.

These changes in the piezoelectric, dielectric and elastic parameters induced by HIP can be analysed from the results shown in Table 3. The reduction of the porosity content after HIP results in an increase of the dielectric permittivity, ε_{33}^{T}, and a reduction of the elastic compliance, s_{11}^{E}, except for PTC-2. These tendencies agree with the previously reported dependence of these parameters:[7,12] the lower the porosity, the higher the permittivity and the lower the elastic compliance. The piezoelectric coefficient d_{33} and the electromechanical coupling factor k_{31} also increase for the HIP ceramics. The improvement of d_{33} with the reduction of the porosity is only noticeable for the HIP ceramics, which are the densest and have the smallest pores. At the same time, no significant changes in the dielectric losses, $\tan\delta$, are observed, in agreement with its independence on variations of microstructural parameters at a mesoscopic scale, such as porosity or grain size.

Regarding the electromechanical coupling factor k_{31}, we expect it to decrease with the reduction of porosity induced by HIP, following the tendency observed in the as-sintered ceramics.[7,12] Previous studies of the k_{31} temperature behaviour have revealed the inversion of the microstructural dependencies at the temperature at which $k_{31}=0$.[12] For the as sintered PTC ceramics this temperature is above room temperature, at which the values shown in Table 3 were obtained. It was also found that the temperature at which $k_{31}=0$ decreases

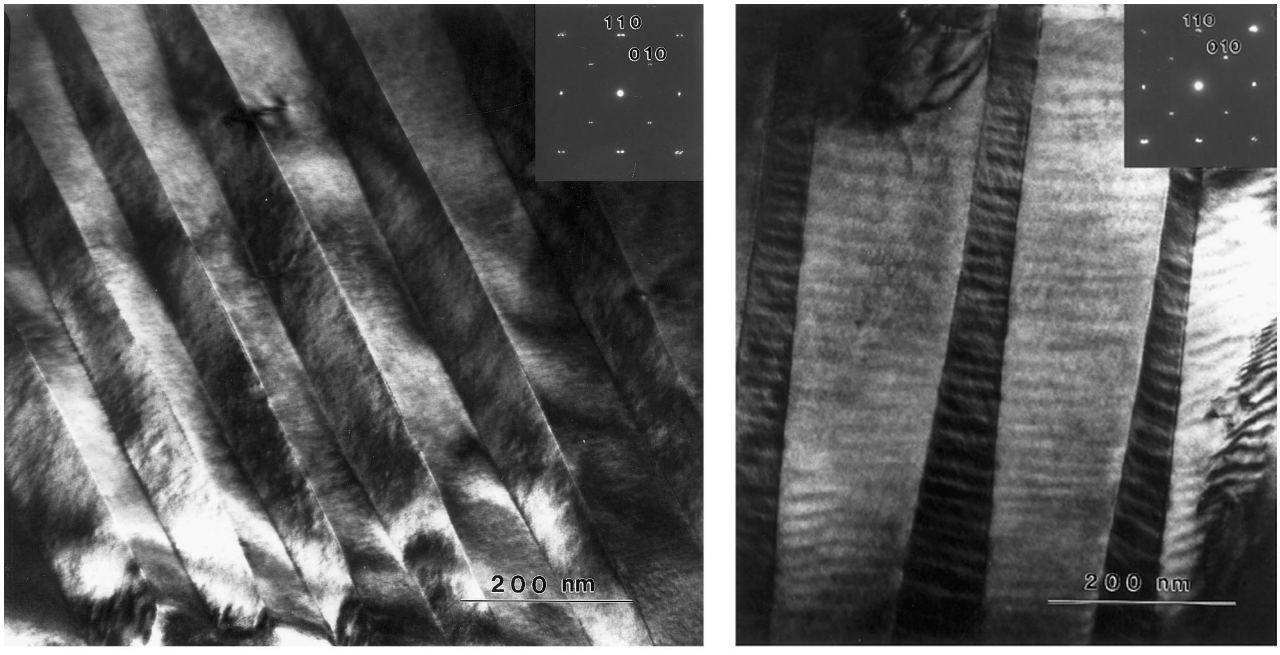

(a) (b)

Fig. 5. Bright field TEM micrographs showing the ferroelectric domain structure of two ceramics before and after HIP: (a) PTC-6 as-sintered; (b) PTC-6 HIP.

Table 3
Piezoelectric, dielectric and elastic parameters at room temperature of HIP treated PTC ceramics, compared to the values for the corresponding as-sintered

PTC ceramic		G (μm)	Poros. (%)	ε_{33}^{T} (1 kHz)	$\tan\delta$ (1 kHz)	d_{33} (pC/N)	k_{31}(%)	s_{11}^{E} (10^{-12} m^2/N)
PTC-2	Sintered	2.3	18.7	167	0.027	57	2.3	9.5
	HIP	1.5	11.3	173	0.040	72	2.3	10.7
PTC-3	Sintered	3.1	7.7	206	0.027	58	0.8	7.8
	HIP	4.3	3.4	228	0.030	69	1.6	6.7
PTC-4	Sintered	3.3	4.7	201	0.029	57	0.9	7.8
	HIP	3.6	0.7	214	0.029	69	1.6	7.0
PTC-6	Sintered	3.9	16.3	185	0.025	60	1.6	8.5
	HIP	3.3	3.1	207	0.028	70	2.1	7.6

with the reduction of the porosity content. The low porosity induced by HIP may reduce this temperature to values below room temperature, inverting the microstructural dependencies of the measured values of k_{31}, and resulting in the observed increase of the values of this parameter.

The ceramic which shows a reduction of the grain size after HIP, PTC-2 HIP, presents with respect to the as-sintered an important change in tanδ, an anomalously high d_{33} and an increase in the elastic compliance s_{11}^{E} opposite to the trend of the rest of the series. The suggested appearance of fractured grains in this ceramic will be the origin of the observed dielectric losses, and may alter the mechanical and piezoelectric properties, producing values different to the rest of the analysed HIP samples.

It can be concluded that the dielectric and piezoelectric properties of all the ceramics are generally improved as a result of the HIP treatment regardless of the initial sintering state, due mainly to an important reduction of the porosity in all cases, even when this reduction is much lower for ceramics in early stages of sintering. It is for the last observation that other phenomenon, different from densification, has to be taken into account: the fracture of the grains. This may be avoided by changing the pressure or time of HIP, and can make this post sintering treatment a successful procedure for improving the properties of ferroelectric ceramics sintered in a wide range of conditions.

4. Conclusions

A study of the microstructure and properties improvement of sintered Ca modified lead titanate ceramics by post-sintering HIP has been carried out. The induced changes in the porosity content and the grain and pore sizes are studied quantitatively by the use of probability plots, together with the variations of the ferro-piezoelectric properties are also analysed. The results obtained give a new insight on the effects of the HIP treatment on lead titanate based piezoelectric ceramics sintered under different conditions, and can be summarised as follows:

1. The HIP treatment affects neither the composition of the bulk of the grains nor their crystalline structure, but does affect the microstructure at a mesoscopic scale, i.e. porosity and grain size.
2. The main effect of the HIP treatment is the reduction of the porosity. However the effectiveness of the process is dramatically dependent on the characteristics of the pre-existing porosity, determined by the sintering stage of the initial ceramic:
   a. *Intermediate sintering stage (high porosity content; small and frequently interconnected pores).* HIP achieves only a small reduction of the porosity, affecting mainly the smallest isolated pores. Grain fracture is observed due to the high-pressure gas, which goes inside the ceramic through the interconnected pores.
   b. *Ideal final stage of sintering (porosity constituted by a relatively small number of isolated pores).* For these ceramics, HIP achieves the highest reductions of the porosity content, up to 85%, reaching values of less than 1%.
   c. *Deteriorated final stage of sintering (development of large isolated pores).* HIP has the main effect on the largest pores, allowing the elimination of the pre-existing bimodal character of the pore size distributions, and therefore restoring the deteriorated microstructure.
3. HIP has a small effect on the grain size, with only a moderate increase due to the long treatment time. The ferroelectric domain configuration seems not to be affected by the treatment.
4. The dielectric and piezoelectric properties are improved by HIP due mainly to the reduction of the porosity content. The dielectric permittivity, the piezoelectric coefficient d_{33} and the coupling factor k_{31} increase, and the elastic compliance s_{11}^{E} decreases.

Acknowledgements

Authors wish to thank C.E. Millar and W.W. Wolny (Ferroperm Ltd., Denmark) and C. Fandiño and F. Díaz (Dpto. Materiales Ferroeléctricos ICMM-CSIC, Spain), for the ceramic preparation, and J. Ortiz (ICMM-CSIC, Spain) and D. Gómez (CNM-CSIC, Spain) for their assistance in SEM and EDS. Thanks are also given to Dr. E. Snoeck (CEMES-LOE, CNRS, Toulouse, France) for assistance in TEM results.

References

1. Okada, N., Ishikawa, K., Murakami, K., Nomura, T., Hagino, M., Nishino, N. and Kihara, U., Microstructure of alkoxide-prepared lead zirconate titanate actuator. *Jpn. J. Appl. Phys. Part 1*, 1992, **31**(9B), 3041–3044.
2. Adachi, M., Toshima, T., Yachizaka, J. and Kawabata, A., Preparation and properties of $Pb(Sc_{1/2}Nb_{1/2})O_3$–$Pb_{00.85}La_{0.15}$-$Ti_{0.96}O_3$ (PSN–PLT) solid-solution ceramics. *Jpn. J. Appl. Phys. Part 1*, 1996, **35**(9B), 5094–5098.
3. Damjanovic, D., Wolny, W., Engan, H., Lethiecq, M. and Pardo, L., Properties and applications of modified lead titanate ceramics. In *Proceedings of the IEEE International Frequency Control Symposium*, 1998, pp. 770–778.
4. Levassort, F., Lethiecq, M., Tran-Huu-Hue, L. P. and Wolny, W., High frequency properties of new fine grained modified lead titanate ceramics. In *Proceedings of the IEEE International Ultrasonics Symposium,* 1997, pp. 947–950.
5. Ito, Y., Nagatsuma, K., Takeuchi, H. and Jyomura, S., Surface

acoustic wave and piezoelectric properties of (Pb,Ln)(TiMn)O_3 ceramics (Ln = rare earths). *J. Appl. Phys*., 1981, **52**(7), 4479–4486.
6. Ricote, J. and Pardo, L., Microstructure-properties relationships in samarium modified lead titanate piezoceramics Part I: quantitative study of the microstructure. *Acta Mater*., 1996, **44**(3), 1155–1167.
7. Ricote, J., Alemany, C., Pardo, L. and Millar, C. E., Microstructure-properties relationships in samarium modified lead titanate piezoceramics Part II: dielectric, piezoelectric and mechanical properties. *Acta Mater*., 1996, **44**(3), 1169–1179.
8. Millar, C. E., Wolny, W., Ricote, J., Alemany, C. and Pardo, L., The effect of hot isostatic pressing on the microstructure of hydrothermally processed $PbTiO_3$ ceramics. *British Ceramic Proc*., 1994, **52**, 185–193.
9. Millar, C. E., Pedersen, L., Pardo, L., Ricote, J., Alemany, C., Jiménez, B., Feuillard, G. and Lethiecq, M., Effect of processing on surface acoustic waves properties of a modified lead titanate ceramic. In *Proceedings of the 9th International Symposium of Applications on Ferroelectrics, (ISAF-94)*, 1994, pp. 138–141.
10. Kwon, S. T. and Kim, D. Y., Effect of sintering temperature on the densification of Al_2O_3. *J. Am. Ceram. Soc*., 1987, **70**(4), C69–C70.
11. del Olmo, L., Pardo, L., Jiménez, B. and Mendiola, J., Piezoelectric behaviour of $Pb_{1-x}Ca_xTiO_3$ ceramics obtained by reactive processes. *Ferroelectrics*, 1988, **81**, 293–296.
12. Ricote, J., Alemany, C. and Pardo, L., Microstructural effects on dielectric and piezoelectric behaviour of calcium-modified lead titanate ceramics. *J. Mater. Res*., 1995, **10**(12), 3194–3203.
13. Allen, T., *Particle Size Measurement*. Chapman and Hall, London, 1981 (Chapter 4).
14. Alemany, C., Pardo, L., Jiménez, B., Carmona, F., Mendiola, J. and González, A. M., Automatic iterative evaluation of complex material constants in piezoelectric ceramics. *J. Phys. D: Appl., Phys*., 1994, **27**, 148–155.
15. Verwerft, M., Van Tendeloo, G., Van Landuyt, J. and Amelinckx, S., Electron microscopy of domain structures. *Ferroelectrics*, 1989, **97**, 5–17.